



# TECH BRIEFS

NATIONAL AERONAUTICS AND SPACE ADMINISTRATION

-  Technology Focus
-  Electronics/Computers
-  Software
-  Materials
-  Mechanics/Machinery
-  Manufacturing
-  Bio-Medical
-  Physical Sciences
-  Information Sciences
-  Books and Reports



# INTRODUCTION

Tech Briefs are short announcements of innovations originating from research and development activities of the National Aeronautics and Space Administration. They emphasize information considered likely to be transferable across industrial, regional, or disciplinary lines and are issued to encourage commercial application.

## Availability of NASA Tech Briefs and TSPs

Requests for individual Tech Briefs or for Technical Support Packages (TSPs) announced herein should be addressed to

### National Technology Transfer Center

Telephone No. **(800) 678-6882** or via World Wide Web at **[www.nttc.edu](http://www.nttc.edu)**

Please reference the control numbers appearing at the end of each Tech Brief. Information on NASA's Innovative Partnerships Program (IPP), its documents, and services is also available at the same facility or on the World Wide Web at **<http://www.nasa.gov/offices/ipp/network/index.html>**

Innovative Partnerships Offices are located at NASA field centers to provide technology-transfer access to industrial users. Inquiries can be made by contacting NASA field centers listed below.

Ames Research Center  
Lisa L. Lockyer  
(650) 604-1754  
[lisa.l.lockyer@nasa.gov](mailto:lisa.l.lockyer@nasa.gov)

Dryden Flight Research Center  
Yvonne D. Gibbs  
(661) 276-3720  
[yvonne.d.gibbs@nasa.gov](mailto:yvonne.d.gibbs@nasa.gov)

Glenn Research Center  
Kathy Needham  
(216) 433-2802  
[kathleen.k.needham@nasa.gov](mailto:kathleen.k.needham@nasa.gov)

Goddard Space Flight Center  
Nona Cheeks  
(301) 286-5810  
[nona.k.cheeks@nasa.gov](mailto:nona.k.cheeks@nasa.gov)

Jet Propulsion Laboratory  
Andrew Gray  
(818) 354-4906  
[gray@jpl.nasa.gov](mailto:gray@jpl.nasa.gov)

Johnson Space Center  
information  
(281) 483-3809  
[jsc.techtran@mail.nasa.gov](mailto:jsc.techtran@mail.nasa.gov)

Kennedy Space Center  
David R. Makufka  
(321) 867-6227  
[david.r.makufka@nasa.gov](mailto:david.r.makufka@nasa.gov)

Langley Research Center  
Elizabeth B. Plentovich  
(757) 864-2857  
[elizabeth.b.plentovich@nasa.gov](mailto:elizabeth.b.plentovich@nasa.gov)

Marshall Space Flight Center  
Jim Dowdy  
(256) 544-7604  
[jim.dowdy@msfc.nasa.gov](mailto:jim.dowdy@msfc.nasa.gov)

Stennis Space Center  
Ramona Travis  
(228) 688-3832  
[ramona.e.travis@nasa.gov](mailto:ramona.e.travis@nasa.gov)

Carl Ray, Program Executive  
Small Business Innovation  
Research (SBIR) & Small  
Business Technology  
Transfer (STTR) Programs  
(202) 358-4652  
[carl.g.ray@nasa.gov](mailto:carl.g.ray@nasa.gov)

Doug Comstock, Director  
Innovative Partnerships  
Program Office  
(202) 358-2221  
[doug.comstock@nasa.gov](mailto:doug.comstock@nasa.gov)





# TECH BRIEFS

NATIONAL AERONAUTICS AND SPACE ADMINISTRATION



## 5 Technology Focus: Electronic Components

- 5 Coherent Frequency Reference System for the NASA Deep Space Network
- 5 Diamond Heat-Spreader for Submillimeter-Wave Frequency Multipliers
- 6 180-GHz I-Q Second Harmonic Resistive Mixer MMIC
- 6 Ultra-Low-Noise W-Band MMIC Detector Modules
- 6 338-GHz Semiconductor Amplifier Module
- 6 Power Amplifier Module With 734-mW Continuous Wave Output Power



## 9 Electronics/Computers

- 9 Multiple Differential-Amplifier MMICs Embedded in Waveguides
- 9 Rapid Corner Detection Using FPGAs
- 10 Special Component Designs for Differential-Amplifier MMICs
- 10 Multi-Stage System for Automatic Target Recognition
- 11 Single-Receiver GPS Phase Bias Resolution
- 12 Ultra-Wideband Angle-of-Arrival Tracking Systems
- 13 Update on Waveguide-Embedded Differential MMIC Amplifiers



## 15 Software

- 15 Automation Framework for Flight Dynamics Products Generation
- 15 Product Operations Status Summary Metrics
- 15 Mars Terrain Generation
- 15 Application-Controlled Parallel Asynchronous Input/Output Utility
- 16 Planetary Image Geometry Library



## 17 Manufacturing & Prototyping

- 17 Propulsion Design With Freeform Fabrication (PDF)
- 17 Economical Fabrication of Thick-Section Ceramic Matrix Composites
- 18 Process for Making a Noble Metal on Tin Oxide Catalyst



## 19 Mechanics/Machinery

- 19 Stacked Corrugated Horn Rings
- 19 Refinements in an Mg/MgH<sub>2</sub>/H<sub>2</sub>O-Based Hydrogen Generator
- 20 Continuous/Batch Mg/MgH<sub>2</sub>/H<sub>2</sub>O-Based Hydrogen Generator
- 21 Strain System for the Motion Base Shuttle Mission Simulator
- 21 Ko Displacement Theory for Structural sShape Predictions
- 22 Pyrotechnic Actuator for Retracting Tubes Between MSL Subsystems



## 23 Physical Sciences

- 23 Surface-Enhanced X-Ray Fluorescence
- 24 Infrared Sensor on Unmanned Aircraft Transmits Time-Critical Wildfire Data
- 24 Slopes To Prevent Trapping of Bubbles in Microfluidic Channels

This document was prepared under the sponsorship of the National Aeronautics and Space Administration. Neither the United States Government nor any person acting on behalf of the United States Government assumes any liability resulting from the use of the information contained in this document, or warrants that such use will be free from privately owned rights.





## Coherent Frequency Reference System for the NASA Deep Space Network

*NASA's Jet Propulsion Laboratory, Pasadena, California*

The NASA Deep Space Network (DSN) requires state-of-the-art frequency references that are derived and distributed from very stable atomic frequency standards. A new Frequency Reference System (FRS) and Frequency Reference Distribution System (FRD) have been developed, which together replace the previous Coherent Reference Generator System (CRG). The FRS and FRD each provide new capabilities that significantly improve operability and reliability.

The FRS allows for selection and switching between frequency standards, a flywheel capability (to avoid interruptions when switching frequency stan-

dards), and a frequency synthesis system (to generate standardized 5-, 10-, and 100-MHz reference signals). The FRS is powered by redundant, specially filtered, and sustainable power systems and includes a monitor and control capability for station operations to interact and control the frequency-standard selection process. The FRD receives the standardized 5-, 10-, and 100-MHz reference signals and distributes signals to distribution amplifiers in a fan out fashion to dozens of DSN users that require the highly stable reference signals. The FRD is also powered by redundant, specially filtered, and sustainable power systems.

The new DSN Frequency Distribution System, which consists of the FRS and FRD systems described here, is central to all operational activities of the NASA DSN. The frequency generation and distribution system provides ultra-stable, coherent, and very low phase-noise references at 5, 10, and 100 MHz to between 60 and 100 separate users at each Deep Space Communications Complex.

*This work was done by Blake C. Tucker, John E. Lauf, Robert L. Hamell, Jorge Gonzalez, Jr., William A. Diener, and Robert L. Tjoelker of Caltech for NASA's Jet Propulsion Laboratory. For more information, contact iaoffice@jpl.nasa.gov. NPO-46602*

## Diamond Heat-Spreader for Submillimeter-Wave Frequency Multipliers

**Superior thermal management provides a 100-percent increase in power-handling capability.**

*NASA's Jet Propulsion Laboratory, Pasadena, California*

The planar GaAs Shottky diode frequency multiplier is a critical technology for the local oscillator (LO) for submillimeter-wave heterodyne receivers due to low mass, tenability, long lifetime, and room-temperature operation. The use of a W-band (75–100 GHz) power amplifier followed by a frequency multiplier is the most common for submillimeter-wave sources. Its greatest challenge is to provide enough input power to the LO for instruments onboard future planetary missions.

Recently, JPL produced 800 mW at 92.5 GHz by combining four MMICs in parallel in a balanced configuration. As more power at W-band is available to the multipliers, their power-handling capability becomes more important. High operating temperatures can lead to degradation of conversion efficiency or catastrophic failure.

The goal of this innovation is to reduce the thermal resistance by attaching diamond film as a heat-spreader on the backside of multipliers to improve their

power-handling capability. Polycrystalline diamond is deposited by hot-filament chemical vapor deposition (CVD). This diamond film acts as a heat-spreader to both the existing 250- and 300-GHz triplers, and has a high thermal conductivity (1,000–1,200 W/mK). It is approximately 2.5 times greater than copper (401 W/mK) and 20 times greater than GaAs (46 W/mK). It is an electrical insulator (resistivity  $\approx 10^{15}$   $\Omega$ -cm), and has a low relative dielectric constant of 5.7.

Diamond heat-spreaders reduce by at least 200 °C at 250 mW of input power, compared to the tripler without diamond, according to thermal simulation. This superior thermal management provides a 100-percent increase in power-handling capability. For example, with this innovation, 40-mW output power has been achieved from a 250-GHz tripler at 350-mW input power, while the previous triplers, without diamond, suffered catastrophic failures. This breakthrough provides a stepping-stone for

frequency multipliers-based LO up to 3 THz. The future work for this design is to apply the high output power from both the 250 and 300 GHz to multiple chains in order to generate milliwatts at 2–3 THz.

Using the first generation of results for this innovation, 40 mW of output power were produced from a 240-GHz tripler at 350-mW input power, and 27-mW output power was produced from a 300-GHz tripler at 408-mW input power. This is two times higher than the current state-of-the-art output power capability. A finite-element thermal simulation also shows that 30- $\mu$ m thick diamond dropped the temperature of the anodes by at least 200 °C.

*This work was done by Robert H. Lin, Erich T. Schlecht, Goutam Chattopadhyay, John J. Gill, Imran Mehdi, Peter H. Siegel, John S. Ward, Choonsup Lee, and Bertrand C. Thomas of Caltech and Alain Maestrini of University Pierre et Marie Curie Paris for NASA's Jet Propulsion Laboratory. For more information, contact iaoffice@jpl.nasa.gov. NPO-46777.*

---

## 180-GHz I-Q Second Harmonic Resistive Mixer MMIC

*NASA's Jet Propulsion Laboratory, Pasadena, California*

An indium phosphide MMIC (monolithic microwave integrated circuit) mixer was developed, processed, and tested in the NGC 35-nm-gate-length HEMT (high electron mobility transistor) process. The MMIC mixers were tested and assembled in the miniature MMIC receiver module described in "Miniature Low-Noise G-Band

I-Q Receiver" (NPO-47442), *NASA Tech Briefs*, Vol. 34, No. 11 (November 2010), p. 45. This innovation is very compact in size and operates with very low LO power. Because it is a resistive mixer, this innovation does not require DC power. This is an enabling technology for the miniature receiver modules for the GeoSTAR instru-

ment, which is the only viable option for the NRC decadal study mission PATH.

*This work was done by Pekka P. Kangaslahti of Caltech and Richard Lai and Xiaobing Mei of Northrop Grumman Corporation for NASA's Jet Propulsion Laboratory. For more information, contact iaoffice@jpl.nasa.gov. NPO-47443*

---

## Ultra-Low-Noise W-Band MMIC Detector Modules

*NASA's Jet Propulsion Laboratory, Pasadena, California*

A monolithic microwave integrated circuit (MMIC) receiver can be used as a building block for next-generation radio astronomy instruments that are scalable to hundreds or thousands of pixels. W-band (75–110 GHz) low-noise receivers are needed for radio astronomy interferometers and spectrometers, and can be used in missile radar and security imagers.

These receivers need to be designed to be mass-producible to increase the sensitivity of the instrument. This innovation is a prototyped single-sideband MMIC receiver that has all the receiver front-end functionality in one small and planar module. The planar module is easy to assemble in volume and does not require tuning of individual receivers. This makes this design low-cost in large volumes.

*This work was done by Todd C. Gaier, Lorene A. Samoska, and Pekka P. Kangaslahti of Caltech; Dan Van Vinkle, Sami Tantawi, John Fox, Sarah E. Church, Judy M. Lau, Matthew M. Sieth, and Patricia E. Voll of Stanford University; and Eric Bryerton of NRAO for NASA's Jet Propulsion Laboratory. Further information is contained in a TSP (see page 1). NPO-47348*

---

## 338-GHz Semiconductor Amplifier Module

*NASA's Jet Propulsion Laboratory, Pasadena, California*

A 35-nm-gate-length InP, high-electron-mobility transistor (HEMT) with a high-indium-content channel as the key component was developed to produce an MMIC (monolithic microwave integrated circuit) power amplifier. With a shorter gate length than previous transistor generations, it allows for electrons to travel shorter distances. This results in higher frequency functionality. In addition, the fabrication process provides for a comprehensive passive component library of resistors, capaci-

tors, airbridge wiring, and through-wafer vias that allow for transistor RF matching and power combining on-chip, making the measured 10-mW 338-GHz chip possible.

The amplifier module can be used in series with current  $\approx 340$  GHz RF sources to boost RF output power. The extremely high-frequency power amplifier module can be used for very-high-frequency wide-bandwidth communication, and higher resolution radars for civilian applications.

*This work was done by Lorene A. Samoska, Todd C. Gaier, Mary M. Soria, and King Man Fung of Caltech and Vesna Radisic, William Deal, Kevin Leong, Xiao Bing Mei, Wayne Yoshida, Po-Hsin Liu, Jansen Uyeda, and Richard Lai of Northrop Grumman Corp. for NASA's Jet Propulsion Laboratory.*

*The software used in this innovation is available for commercial licensing. Please contact Daniel Broderick of the California Institute of Technology at danielb@caltech.edu. Refer to NPO-47307.*

---

## Power Amplifier Module With 734-mW Continuous Wave Output Power

*NASA's Jet Propulsion Laboratory, Pasadena, California*

Research findings were reported from an investigation of new gallium nitride (GaN) monolithic millimeter-wave integrated circuit (MMIC) power amplifiers

(PAs) targeting the highest output power and the highest efficiency for class-A operation in W-band (75–110 GHz). W-band PAs are a major component of many fre-

quency multiplied submillimeter-wave LO signal sources. For spectrometer arrays, substantial W-band power is required due to the passive lossy frequency multipliers

used to generate higher frequency signals in nonlinear Schottky diode-based LO sources. By advancing PA technology, the LO system performance can be increased with possible cost reductions compared to current GaAs PAs.

High-power, high-efficiency GaN PAs are cross-cutting and can enable more

efficient local oscillator distribution systems for new astrophysics and planetary receivers and heterodyne array instruments. It can also allow for a new, electronically scannable solid-state array technology for future Earth science radar instruments and communications platforms.

*This work was done by King Man Fung, Lorene A. Samoska, Pekka P. Kangaslahti, Bjorn H. Lambriksen, Paul F. Goldsmith, Robert H. Lin, Mary M. Soria, and Joelle T. Cooperrider of Caltech and Miroslav Micovic and Ara Kurdoghlian of HRL Laboratories for NASA's Jet Propulsion Laboratory. Further information is contained in a TSP (see page 1). NPO-47364*





### Multiple Differential-Amplifier MMICs Embedded in Waveguides

Amplifiers are separated by no more than fractional-wavelength distances.

NASA's Jet Propulsion Laboratory, Pasadena, California

Compact amplifier assemblies of a type now being developed for operation at frequencies of hundreds of gigahertz comprise multiple amplifier units in parallel arrangements to increase power and/or cascade arrangements to increase gains. Each amplifier unit is a monolithic microwave integrated circuit (MMIC) implementation of a pair of amplifiers in differential (in contradistinction to single-ended) configuration.

Heretofore, in cascading amplifiers to increase gain, it has been common practice to interconnect the amplifiers by use of wires and/or thin films on substrates. This practice has not yielded satisfactory results at frequencies >200 Hz, in each case, for either or both of two reasons:

- Wire bonds introduce large discontinuities.
- Because the interconnections are typically tens of wavelengths long, any impedance mismatches give rise to ripples in the gain-vs.-frequency response, which degrade the performance of the cascade.

Heretofore, it has been very difficult to achieve net increases in power by combining the outputs of amplifiers at frequencies >100 GHz. The only success-

ful approach that has been even marginally successful has involved the use of waveguide combiners designed and fabricated as components separate from the amplifiers. At these frequencies, even waveguides exhibit high losses that can easily dissipate any power gained by combining outputs.

In the present development, neither thin-film nor wire interconnections are used for cascading, and separate component waveguide combiners are not used for combining power. Instead, the amplifier units are designed integrally with the waveguides and designed to be embedded in the waveguides. The underlying concept of differential-amplifier MMICs designed integrally with and embedded in waveguides and the advantages of the differential over the single-ended configuration were reported in "Differential InP HEMT MMIC Amplifiers Embedded in Waveguides" (NPO-42857) *NASA Tech Briefs*, Vol. 33, No. 9 (September 2009), page 35. The novel aspect of the present development lies in combining the integration and embedment concepts with the cascading and parallel-combining concepts to obtain superior performance. In an amplifier assembly of the present type,

there is no need for interconnecting wires or thin-film conductors nor for separate waveguide power combiners because the waveguide in which the MMICs are embedded is the connecting medium. Because the distance between successive MMICs in a cascade is only a fraction of a wavelength, cascading can be highly efficient and ripple in gain versus frequency is reduced to a minimum. Moreover, power combining can be highly efficient because it is accomplished simply by placing MMICs side by side within the waveguide.

*This work was done by Pekka Kangaslahti and Erich Schlecht of Caltech for NASA's Jet Propulsion Laboratory. For more information, contact iaoffice@jpl.nasa.gov.*

*In accordance with Public Law 96-517, the contractor has elected to retain title to this invention. Inquiries concerning rights for its commercial use should be addressed to:*

*Innovative Technology Assets Management  
JPL*

*Mail Stop 202-233*

*4800 Oak Grove Drive*

*Pasadena, CA 91109-8099*

*E-mail: iaoffice@jpl.nasa.gov*

*Refer to NPO-44394, volume and number of this NASA Tech Briefs issue, and the page number.*

### Rapid Corner Detection Using FPGAs

This algorithm can be used in automotive, navigation, and industrial factory applications.

NASA's Jet Propulsion Laboratory, Pasadena, California

In order to perform precision landings for space missions, a control system must be accurate to within ten meters. Feature detection applied against images taken during descent and correlated against the provided base image is computationally expensive and requires tens of seconds of processing time to do just one image while the goal is to process multiple images per second.

To solve this problem, this algorithm takes that processing load from the central processing unit (CPU) and gives it to a reconfigurable field pro-

grammable gate array (FPGA), which is able to compute data in parallel at very high clock speeds. The workload of the processor then becomes simpler; to read an image from a camera, it is transferred into the FPGA, and the results are read back from the FPGA.

The Harris Corner Detector uses the determinant and trace to find a "corner score," with each step of the computation occurring on independent clock cycles. Essentially, the image is converted into an  $x$  and  $y$  derivative

map. Once three lines of pixel information have been queued up, valid pixel derivatives are clocked into the product and averaging phase of the pipeline. Each  $x$  and  $y$  derivative is squared against itself, as well as the product of the  $i_x$  and  $i_y$  derivative, and each value is stored in a  $W \times N$  size buffer, where  $W$  represents the size of the integration window and  $N$  is the width of the image. In this particular case, a window size of 5 was chosen, and the image is  $640 \times 480$ .

Over a  $W \times N$  size window, an equidis-

tance Gaussian is applied (to bring out the stronger corners), and then each value in the entire window is summed and stored. The required components of the equation are in place, and it is just a matter of taking the determinant and trace. It should be noted that the trace is being weighted by a constant  $\kappa$ , a value that is found empirically to be

within 0.04 to 0.15 (and in this implementation is 0.05). The constant  $\kappa$  determines the number of corners available to be compared against a threshold  $\sigma$  to mark a "valid corner."

After a fixed delay from when the first pixel is clocked in (to fill the pipeline), a score is achieved after each successive clock. This score corresponds with an

$(x,y)$  location within the image. If the score is higher than the predetermined threshold  $\sigma$ , then a flag is set high and the location is recorded.

*This work was done by Arin C. Morfopoulos and Brandon C. Metz of Caltech for NASA's Jet Propulsion Laboratory. Further information is contained in a TSP (see page 1). NPO-47202*

---

## Special Component Designs for Differential-Amplifier MMICs

**Transistors and transmission lines are optimized for differential operation.**

*NASA's Jet Propulsion Laboratory, Pasadena, California*

Special designs of two types of electronic components — transistors and transmission lines — have been conceived to optimize the performances of these components as parts of waveguide-embedded differential-amplifier monolithic microwave integrated circuits (MMICs) of the type described in the immediately preceding article. These designs address the following two issues, the combination of which is unique to these particular MMICs:

- Each MMIC includes a differential double-strip transmission line that typically has an impedance between 60 and 100  $\Omega$ . However, for purposes of matching of impedances, transmission lines having lower impedances are also needed.
- The transistors in each MMIC are, more specifically, one or more pair(s) of InP-based high-electron-mobility transistors (HEMTs). Heretofore, it has been common practice to fabricate each such pair as a single device configured in the side-to-side electrode sequence source/gate/drain/gate/source. This configuration enables low-inductance source grounding from the sides of

the device. However, this configuration is not suitable for differential operation, in which it is necessary to drive the gates differentially and to feed the output from the drain electrodes differentially.

The special transmission-line design provides for three conductors, instead of two, in places where lower impedance is needed. The third conductor is a metal strip placed underneath the differential double-strip transmission line. The third conductor increases the capacitance per unit length of the transmission line by such an amount as to reduce the impedance to between 5 and 15  $\Omega$ .

In the special HEMT-pair design, the side-to-side electrode sequence is changed to drain/gate/source/gate/drain. In addition, the size of the source is reduced significantly, relative to corresponding sizes in prior designs. This reduction is justified by the fact that, by virtue of the differential configuration, the device has an internal virtual ground, and therefore there is no need for a low-resistance contact between the source and the radio-frequency circuitry.

The source contact is needed only for DC biasing.

These designs were implemented in a single-stage-amplifier MMIC. In a test at a frequency of 305 GHz, the amplifier embedded in a waveguide exhibited a gain of 0 dB; after correcting for the loss in the waveguide, the amplifier was found to afford a gain of 0.9 dB. In a test at 220 GHz, the overall gain of the amplifier-and-waveguide assembly was found to be 3.5 dB.

*This work was done by Pekka Kangaslahti of Caltech for NASA's Jet Propulsion Laboratory. For more information, contact [iaoffice@jpl.nasa.gov](mailto:iaoffice@jpl.nasa.gov).*

*In accordance with Public Law 96-517, the contractor has elected to retain title to this invention. Inquiries concerning rights for its commercial use should be addressed to:*

*Innovative Technology Assets Management  
JPL*

*Mail Stop 202-233*

*4800 Oak Grove Drive*

*Pasadena, CA 91109-8099*

*E-mail: [iaoffice@jpl.nasa.gov](mailto:iaoffice@jpl.nasa.gov)*

*Refer to NPO-44393, volume and number of this NASA Tech Briefs issue, and the page number.*

---

## Multi-Stage System for Automatic Target Recognition

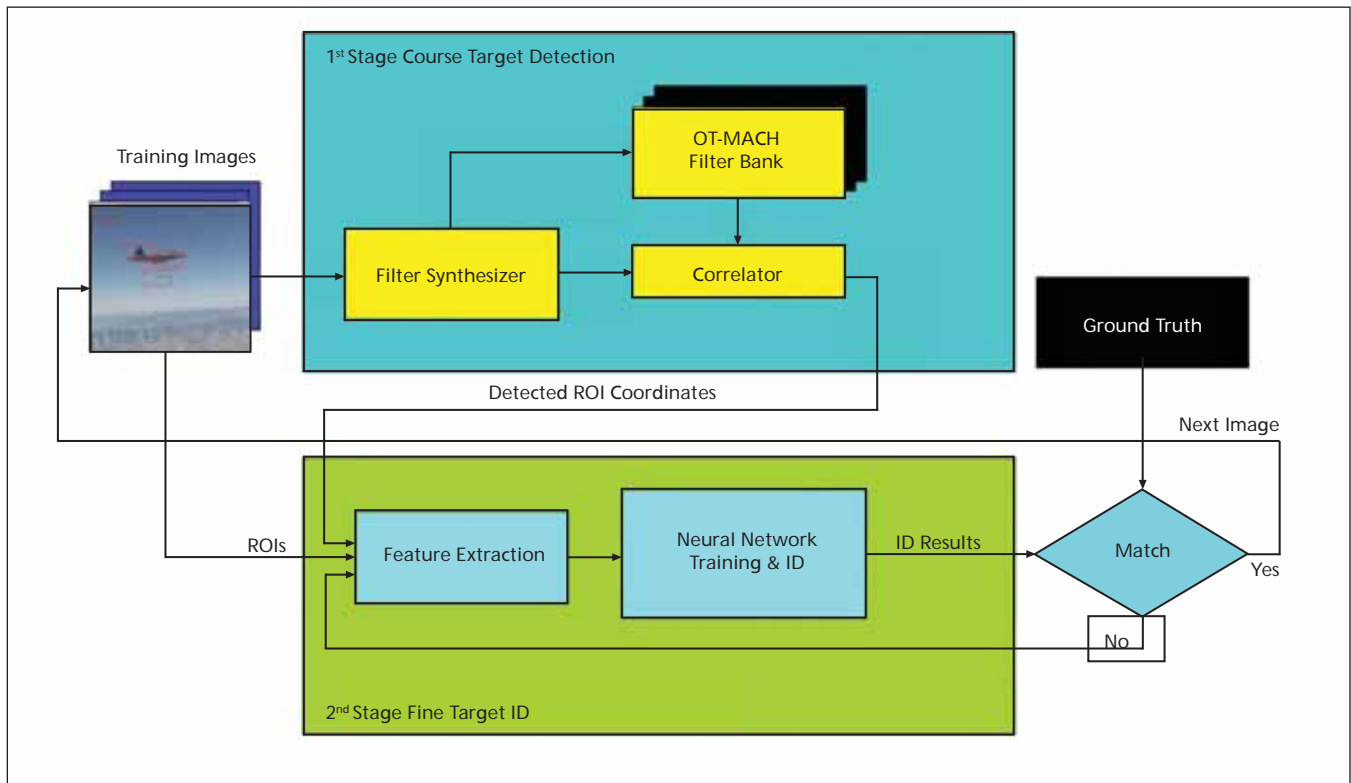
**This system is capable of identifying hazards to avoid in robotic vehicle and automobile navigation.**

*NASA's Jet Propulsion Laboratory, Pasadena, California*

A multi-stage automated target recognition (ATR) system has been designed to perform computer vision tasks with adequate proficiency in mimicking human vision. The system is able to detect, identify, and track targets of interest. Potential regions of interest (ROIs) are first identi-

fied by the detection stage using an Optimum Trade-off Maximum Average Correlation Height (OT-MACH) filter combined with a wavelet transform. False positives are then eliminated by the verification stage using feature extraction methods in conjunction with neural net-

works. Feature extraction transforms the ROIs using filtering and binning algorithms to create feature vectors. A feed-forward back-propagation neural network (NN) is then trained to classify each feature vector and to remove false positives. The system parameter optimiza-



The Multi-Stage ATR System Architecture incorporates a detection stage that first identifies potential ROIs where the target may be present by performing a Fast Fourier domain OT-MACH filter-based correlation.

tions process has been developed to adapt to various targets and datasets.

The objective was to design an efficient computer vision system that can learn to detect multiple targets in large images with unknown backgrounds. Because the target size is small relative to the image size in this problem, there are many regions of the image that could potentially contain the target. A cursory analysis of every region can be computationally efficient, but may yield too many false positives. On the other hand, a detailed analysis of every region can yield better results, but may be computationally inefficient. The multi-stage ATR system was designed to achieve an optimal balance between

accuracy and computational efficiency by incorporating both models.

The detection stage first identifies potential ROIs where the target may be present by performing a fast Fourier domain OT-MACH filter-based correlation. Because threshold for this stage is chosen with the goal of detecting all true positives, a number of false positives are also detected as ROIs. The verification stage then transforms the regions of interest into feature space, and eliminates false positives using an artificial neural network classifier.

The multi-stage system allows tuning the detection sensitivity and the identification specificity individually in each

stage. It is easier to achieve optimized ATR operation based on its specific goal. The test results show that the system was successful in substantially reducing the false positive rate when tested on a sonar and video image datasets.

*This work was done by Tien-Hsin Chao, Thomas T. Lu, and David Ye of Caltech; Weston Edens of Butler University; and Oliver Johnson of Harvey Mudd College for NASA's Jet Propulsion Laboratory. For more information, contact iaoffice@jpl.nasa.gov.*

*The software used in this innovation is available for commercial licensing. Please contact Daniel Broderick of the California Institute of Technology at danielb@caltech.edu. Refer to NPO-47012.*

## Single-Receiver GPS Phase Bias Resolution

NASA's Jet Propulsion Laboratory, Pasadena, California

Existing software has been modified to yield the benefits of integer fixed double-differenced GPS-phased ambiguities when processing data from a single GPS receiver with no access to any other GPS receiver data. When the double-differenced combination of phase biases can be fixed reliably, a sig-

nificant improvement in solution accuracy is obtained.

This innovation uses a large global set of GPS receivers (40 to 80 receivers) to solve for the GPS satellite orbits and clocks (along with any other parameters). In this process, integer ambiguities are fixed and information on the ambi-

guity constraints is saved. For each GPS transmitter/receiver pair, the process saves the arc start and stop times, the wide-lane average value for the arc, the standard deviation of the wide lane, and the dual-frequency phase bias after bias fixing for the arc. The second step of the process uses the orbit and clock infor-

mation, the bias information from the global solution, and only data from the single receiver to resolve double-differenced phase combinations. It is called “resolved” instead of “fixed” because constraints are introduced into the problem with a finite data weight to better account for possible errors.

A receiver in orbit has much shorter continuous passes of data than a receiver fixed to the Earth. The method has pa-

rameters to account for this. In particular, differences in drifting wide-lane values must be handled differently. The first step of the process is automated, using two JPL software sets, Longarc and Gipsy-Oasis. The resulting orbit/clock and bias information files are posted on anonymous ftp for use by any licensed Gipsy-Oasis user. The second step is implemented in the Gipsy-Oasis executable, gd2p.pl, which automates the

entire process, including fetching the information from anonymous ftp.

*This work was done by William I Bertiger, Bruce J. Haines, Jan P. Weiss, and Nathaniel E. Harvey of Caltech for NASA’s Jet Propulsion Laboratory. For more information, contact iaoffice@jpl.nasa.gov.*

*This software is available for commercial licensing. Please contact Daniel Broderick of the California Institute of Technology at danielb@caltech.edu. Refer to NPO-47149.*

## Ultra-Wideband Angle-of-Arrival Tracking Systems

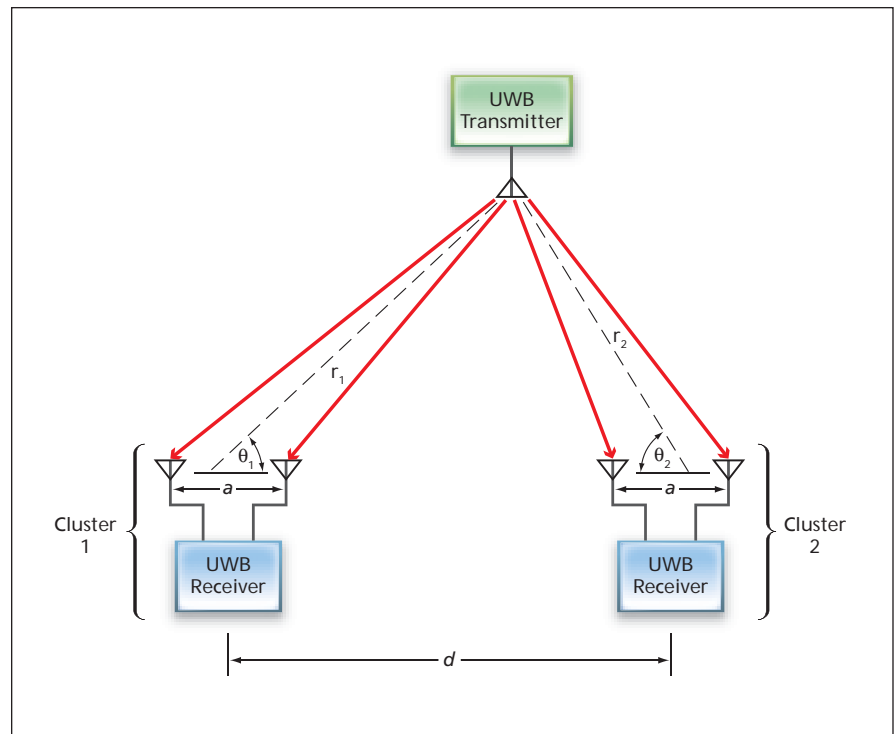
UWB radio pulses afford temporal resolution needed for estimating angles of arrival.

Lyndon B. Johnson Space Center, Houston, Texas

Systems that measure the angles of arrival of ultra-wideband (UWB) radio signals and perform triangulation by use of those angles in order to locate the sources of those signals are undergoing development. These systems were originally intended for use in tracking UWB-transmitter-equipped astronauts and mobile robots on the surfaces of remote planets during early stages of exploration, before satellite-based navigation systems become operational. On Earth, these systems could be adapted to such uses as tracking UWB-transmitter-equipped firefighters inside buildings or in outdoor wildfire areas obscured by smoke.

The same characteristics that have made UWB radio advantageous for fine-resolution ranging, covert communication, and ground-penetrating radar applications in military and law-enforcement settings also contribute to its attractiveness for the present tracking applications. In particular, the waveform shape and the short duration of UWB pulses make it possible to attain the high temporal resolution (of the order of picoseconds) needed to measure angles of arrival with sufficient precision, and the low power spectral density of UWB pulses enables UWB radio communication systems to operate in proximity to other radio communication systems with little or no perceptible mutual interference.

The figure schematically depicts a simple system of this type engaged in tracking a single UWB transmitter on a plane. The system includes two UWB-receiver assemblies, denoted clusters, separated by a known length  $d$ . Within each cluster is a UWB receiver connected to two antennas that are separated by a length  $a$  that is much shorter than the



Angles  $\theta_1$  and  $\theta_2$  are estimated from differences between the times of arrival of UWB radio pulses at the antennas in each cluster. Then using these angles, the relative position of the transmitter is calculated by triangulation.

mentioned length  $d$ . The signals received by the two antennas in each cluster are subjected to a process of cross-correlation plus peak detection to measure differences between their times of arrival. It is assumed that the distances ( $r_1$  and  $r_2$ ) between the clusters and the transmitter are much greater than  $a$ , as would usually be the case in most practical applications. Then the angles of arrival of the signals at the clusters are given by  $\theta_1 \approx \arccos(\tau_1/a)$  and  $\theta_2 \approx \arccos(\tau_2/a)$ ; where  $\theta_1$  and  $\theta_2$  are as shown in the figure;  $c$  is the

speed of light;  $\tau_1$  is the difference between the times of arrival of a pulse at the antennas in cluster 1; and  $\tau_2$  is the difference between the times of arrival of a pulse at the antennas in cluster 2. Then using  $\theta_1$  and  $\theta_2$ , the two-dimensional location of the transmitter, relative to the known locations of the clusters, is calculated straightforwardly by use of the triangulation equations.

The processing of signals to determine the differences between their times of arrival, and the subsequent processing to determine the angles of ar-

rival and the position of the transmitter, is done in a computer external to the clusters. For this purpose, the received waveforms are digitized in the receivers, and the waveform data are sent to the computer via a hub. Even though no attempt is made to synchronize operation of the two receivers, the data from the receivers are quasi-synchronized by means of interface software that effects parallel socket communication with data segmentation, summarized as follows: Waveform data are collected from each receiver in segments, whenever they become available and the computer is

ready to collect them. The segments from each receiver are labeled as having come from that receiver and, in the collection process, are interleaved with those from the other receiver in chronological order of collection. Within the computer, the segments from each receiver are stored in a separate buffer. Thus, the contents of the buffers are representations of the same UWB pulse waveform arriving at the two receivers at approximately the same time. When the buffers for both receivers contain complete representations of a UWB pulse waveform, the data from that buffer are

copied into an array for use in the calculations described above.

*This work was done by G. Dickey Arndt, Phong H. Ngo, Chau T. Phan, and Julia Gross of Johnson Space Center; Jianjun Ni NRC fellow; and John Dusch of Jacobs Sverdrup. Further information is contained in a TSP (see page 1).*

*This invention is owned by NASA, and a patent application has been filed. Inquiries concerning nonexclusive or exclusive license for its commercial development should be addressed to the Patent Counsel, Johnson Space Center, (281) 483-1003. Refer to MSC-24184-1.*

---

## Update on Waveguide-Embedded Differential MMIC Amplifiers

*NASA's Jet Propulsion Laboratory, Pasadena, California*

There is an update on the subject matter of "Differential InP HEMT MMIC Amplifiers Embedded in Waveguides" (NPO-42857) *NASA Tech Briefs*, Vol. 33, No. 9 (September 2009), page 35. To recapitulate: Monolithic microwave integrated-circuit (MMIC) amplifiers of a type now being developed for operation at frequencies of hundreds of gigahertz contain InP high-electron-mobility transistors (HEMTs) in a differential configuration. The MMICs are designed integrally with, and embedded in, waveguide packages. The instant work does not mention InP HEMTs but otherwise reiterates part of the subject matter of the cited prior article, with emphasis on the following salient points:

- An MMIC is mounted in the electric-field plane ("E-plane") of a waveguide and includes a finline transition to each differential-amplifier stage.
- The differential configuration creates a virtual ground within each pair of transistor-gate fingers, eliminating the need for external radio-frequency grounding.

This work concludes by describing a single-stage differential submillimeter-wave amplifier packaged in a rectangular waveguide and summarizing results of tests of this amplifier at frequencies of 220 and 305 GHz.

*This work was done by Pekka Kangaslahti and Erich Schlecht of Caltech for NASA's Jet*

*Propulsion Laboratory. For more information, contact [iaoffice@jpl.nasa.gov](mailto:iaoffice@jpl.nasa.gov).*

*In accordance with Public Law 96-517, the contractor has elected to retain title to this invention. Inquiries concerning rights for its commercial use should be addressed to:*

*Innovative Technology Assets Management  
JPL*

*Mail Stop 202-233*

*4800 Oak Grove Drive*

*Pasadena, CA 91109-8099*

*E-mail: [iaoffice@jpl.nasa.gov](mailto:iaoffice@jpl.nasa.gov)*

*Refer to NPO-44401, volume and number of this NASA Tech Briefs issue, and the page number.*





## Automation Framework for Flight Dynamics Products Generation

XFDS provides an easily adaptable automation platform. To date it has been used to support flight dynamics operations. It coordinates the execution of other applications such as Satellite TookKit, FreeFlyer, MATLAB, and Perl code. It provides a mechanism for passing messages among a collection of XFDS processes, and allows sending and receiving of GMSEC messages. A unified and consistent graphical user interface (GUI) is used for the various tools. Its automation configuration is stored in text files, and can be edited either directly or using the GUI.

XFDS is implemented as a group of cooperating processes. One process coordinates communications, another drives an optional GUI (not needed if running in batch mode), and the rest carry out automation tasks. The software is designed around three concepts: (1) an "action" controls an automation step; (2) a "variable" allows information to be shared among actions; and (3) a "form" corresponds to a GUI widget, which can be reused between action editors.

A significant strength of this approach is to provide a high-level abstraction to the procedures that need to be carried out. Frequently changed parameters are readily available for modification, while the rest are hidden. Additional programs that provide a batch interface can be added to this system.

*This work was done by Robert E. Wiegand, Timothy C. Esposito, John S. Watson, Linda Jun, Wendy Shoan, and Carla Matusow of Goddard Space Flight Center and Wayne McCullough of Computer Sciences Corp. For further information, contact the Goddard Innovative Partnerships Office at (301) 286-5810. GSC-15618-1.*

## Product Operations Status Summary Metrics

The Product Operations Status Summary Metrics (POSSUM) computer program provides a readable view into the state of the Phoenix Operations Product Generation Subsystem (OPGS) data pipeline. POSSUM provides a user interface that can search the data store, collect

product metadata, and display the results in an easily-readable layout. It was designed with flexibility in mind for support in future missions. Flexibility over various data store hierarchies is provided through the disk-searching facilities of Marsviewer. This is a proven program that has been in operational use since the first day of the Phoenix mission.

POSSUM presents a graphical representation for tracking and accountability of the existence and version of expected Reduced Data Records (RDRs) for a given Experiment Data Record (EDR) for the Phoenix lander mission. By using POSSUM, operations personnel can easily determine if any RDRs are missing for a given EDR during and after OPGS processing pipeline. A variety of sort options exists, including product file creation time and instrument.

*This work was done by Atsuya Takagi and Nicholas Toole of Caltech for NASA's Jet Propulsion Laboratory.*

*The software used in this innovation is available for commercial licensing. Please contact Daniel Broderick of the California Institute of Technology at danielb@caltech.edu. Refer to NPO-46664.*

## Mars Terrain Generation

A suite of programs for the generation of disparity maps from stereo image pairs via correlation, and conversion of those disparity maps to XYZ maps, has been updated. This suite implements an automated method of deriving terrain from stereo images for use in the ground data system for *in-situ* (lander and rover) cameras. This differs from onboard correlation by concentrating more on accuracy than speed, since near-real-time is not a requirement on the ground. The final result is an XYZ value for every point in the image that passes several quality checks. *A priori* geometric camera calibration information is required for this suite to operate.

The suite is very flexible, enabling its use in many special situations, such as non-linearized images required for applications like the Phoenix arm camera, or long-baseline stereo, where the rover moves between left and right images. The suite consists of:

- marscor3: The primary correlation program used by MER, PHX, and (soon) MSL. Requires a low-resolution

disparity map as input, and refines it.

- marsjplstereo: A wrapper around a much faster correlator that assumes the images are epipolar aligned ("linearized"). Creates the input for marscor3.
- marsunlinearize: Takes a linearized correlation result and unprojects it back to raw geometry. Creates the input for marscor3 in some non-linearized situations.
- marsfakedisp: Creates the input for marscor3 in some non-linearized cases by assuming an approximate surface.
- marsdispinvert: "Inverts" a disparity map (e.g., from L→R to R→L) to create an input for marscor3.
- marsxyz: Takes the disparity map (e.g., from marscor3) and generates XYZ coordinates for each pixel.
- marsfilter: Filters the output of marsxyz to mask off undesirable areas (such as the rover itself, horizon, etc.).
- marsrange: Takes the results from marsxyz and computes range from the camera for each pixel.

While the underlying correlation coefficient computation is nearly the same as in the original, the algorithms driving how that correlation is accomplished have been completely redesigned. In addition, significant new capability exists, such as non-linearized stereo, R→L inversion, masking, and range computation. Significant additions to marsxyz's filtering capability to reject bad correlations have also been made.

*This work was done by Robert G. Deen of Caltech for NASA's Jet Propulsion Laboratory.*

*This software is available for commercial licensing. Please contact Daniel Broderick of the California Institute of Technology at danielb@caltech.edu. Refer to NPO-46659.*

## Application-Controlled Parallel Asynchronous Input/Output Utility

A software utility tool has been designed to alleviate file system I/O performance bottlenecks to which many high-end computing (HEC) applications fall prey because of the relatively large volume of data generated for a given amount of computational work. In an effort to reduce computing resource waste, and to improve sustained performance of these HEC applications, a lightweight software utility has been de-

signed to circumvent bandwidth limitations of typical HEC file systems by exploiting the faster inter-processor bandwidth to move output data from compute nodes to designated I/O nodes as quickly as possible, thereby minimizing the I/O wait time. This utility has successfully demonstrated a significant performance improvement within a major NASA weather application.

*This work was done by Thomas Clune of Goddard Space Flight Center and Shujia Zhou of Northrop Grumman. For further information, contact the Goddard Innovative Partnerships Office at (301) 286-5810. GSC-15751-1*

---

## **Planetary Image Geometry Library**

The Planetary Image Geometry (PIG) library is a multi-mission library used for projecting images (EDRs, or Experiment Data Records) and managing their geometry for *in-situ* missions. A collection of models describes cameras and their articulation, allowing application programs such as mosaickers, terrain generators, and pointing correc-

tion tools to be written in a multi-mission manner, without any knowledge of parameters specific to the supported missions.

Camera model objects allow transformation of image coordinates to and from view vectors in XYZ space. Pointing models, specific to each mission, describe how to orient the camera models based on telemetry or other information. Surface models describe the surface in general terms. Coordinate system objects manage the various coordinate systems involved in most missions. File objects manage access to metadata (labels, including telemetry information) in the input EDRs and RDRs (Reduced Data Records). Label models manage metadata information in output files. Site objects keep track of different locations where the spacecraft might be at a given time. Radiometry models allow correction of radiometry for an image. Mission objects contain basic mission parameters. Pointing adjustment (“nav”) files allow pointing to be corrected.

The object-oriented structure (C++) makes it easy to subclass just the pieces

of the library that are truly mission-specific. Typically, this involves just the pointing model and coordinate systems, and parts of the file model. Once the library was developed (initially for Mars Polar Lander, MPL), adding new missions ranged from two days to a few months, resulting in significant cost savings as compared to rewriting all the application programs for each mission. Currently supported missions include Mars Pathfinder (MPF), MPL, Mars Exploration Rover (MER), Phoenix, and Mars Science Lab (MSL). Applications based on this library create the majority of operational image RDRs for those missions. A Java wrapper around the library allows parts of it to be used from Java code (via a native JNI interface). Future conversions of all or part of the library to Java are contemplated.

*This work was done by Robert G. Deen and Oleg Pariser of Caltech for NASA's Jet Propulsion Laboratory.*

*The software used in this innovation is available for commercial licensing. Please contact Daniel Broderick of the California Institute of Technology at [danielb@caltech.edu](mailto:danielb@caltech.edu). Refer to NPO-46658.*



## Propulsion Design With Freeform Fabrication (PDFF)

**Innovation for ceramic materials uses solid freeform rapid prototype manufacturing technology.**

*John H. Glenn Research Center, Cleveland, Ohio*

The nation is challenged to decrease the cost and schedule to develop new space transportation propulsion systems for commercial, scientific, and military purposes. Better design criteria and manufacturing techniques for small thrusters are needed to meet current applications in missile defense, space, and satellite propulsion. The requirements of these systems present size, performance, and environmental demands on these thrusters that have posed significant challenges to the current designers and manufacturers. Designers are limited by manufacturing processes, which are complex, costly, and time consuming, and ultimately limited in their capabilities.

The PDFF innovation vastly extends the design opportunities of rocket engine components and systems by making use of the unique manufacturing freedom of solid freeform rapid prototype manufacturing technology combined with the benefits of ceramic materials. The unique features of PDFF are developing and implementing a design methodology that uses solid freeform fabrication (SFF) techniques to make propulsion components with

significantly improved performance, thermal management, power density, and stability, while reducing development and production costs. PDFF extends the design process envelope beyond conventional constraints by leveraging the key feature of the SFF technique with the capability to form objects with nearly any geometric complexity without the need for elaborate machine setup. The marriage of SFF technology to propulsion components allows an evolution of design practice to harmonize material properties with functional design efficiency.

Reduced density of materials when coupled with the capability to honeycomb structure used in the injector will have significant impact on overall mass reduction. Typical thrusters in use for attitude control have 60–90 percent of its mass in the valve and injector, which is typically made from titanium. The combination of material and structure envisioned for use in an SFF thruster design could reduce thruster weight by a factor of two or more. The thrust-to-weight ratios for such designs can achieve 1,000:1 or more, depending on chamber pressure.

The potential exists for continued development in materials, size, speed, accuracy of SFF techniques, which can lead to speculative developments of PDFF processes such as fabrication of custom human interface devices like masks, chairs, and clothing, and advanced biomedical application to human organ reconstruction.

Other potential applications are: higher fidelity lower cost test fixtures for probes and inspection, disposable thrusters, and ISRU (*in situ* resource utilization) for component production in space or on Lunar and Martian missions, and application for embedding MEMS (microelectromechanical systems) during construction process of form changing aerostructure/dynamic structures.

*This work was done by Daudi Barnes of DMX Engineering, Jim McKinnon of Frontier Engineering, and Richard Priem of Priem Consultants for Glenn Research Center. Further information is contained in a TSP (see page 1).*

*Inquiries concerning rights for the commercial use of this invention should be addressed to NASA Glenn Research Center, Innovative Partnerships Office, Attn: Steven Fedor, Mail Stop 4–8, 21000 Brookpark Road, Cleveland, Ohio 44135. Refer to LEW-18557-1.*

## Economical Fabrication of Thick-Section Ceramic Matrix Composites

**Applications for these composites include combustors, high-temperature filter elements, and process industry parts requiring corrosion resistance.**

*Marshall Space Flight Center, Alabama*

A method was developed for producing thick-section [ $>2$  in. ( $\approx 5$  cm)], continuous fiber-reinforced ceramic matrix composites (CMCs). Ultramet-modified fiber interface coating and melt infiltration processing, developed previously for thin-section components, were used for the fabrication of CMCs that were an order of magnitude greater in thickness [up to 2.5 in. ( $\approx 6.4$  cm)]. Melt process-

ing first involves infiltration of a fiber preform with the desired interface coating, and then with carbon to partially densify the preform. A molten refractory metal is then infiltrated and reacts with the excess carbon to form the carbide matrix without damaging the fiber reinforcement. Infiltration occurs from the inside out as the molten metal fills virtually all the available void space. Densifi-

cation to  $<5$  vol% porosity is a one-step process requiring no intermediate machining steps.

The melt infiltration method requires no external pressure. This prevents over-infiltration of the outer surface plies, which can lead to excessive residual porosity in the center of the part. However, processing of thick-section components required modification of the con-

ventional process conditions, and the means by which the large amount of molten metal is introduced into the fiber preform. Modification of the low-temperature, ultraviolet-enhanced chemical vapor deposition process used to apply interface coatings to the fiber preform was also required to accommodate the high preform thickness.

The thick-section CMC processing developed in this work proved to be invaluable for component development, fabrication, and testing in two comple-

mentary efforts. In a project for the Army, involving SiC/SiC blisk development, nominally 0.8 in. thick  $\times$  8 in. diameter ( $\approx$ 2 cm thick  $\times$  20 cm diameter) components were successfully infiltrated. Blisk hubs were machined using diamond-embedded cutting tools and successfully spin-tested. Good ply uniformity and extremely low residual porosity (<2 percent) were achieved, the latter being far lower than that achieved with SiC matrix composites fabricated via CVI or PIP. The pyrolytic

carbon/zirconium nitride interface coating optimized in this work for use on carbon fibers was incorporated in the SiC/SiC composites and yielded a >41 ksi ( $\approx$ 283 MPa) flexural strength.

*This work was done by Jason Babcock, Gautham Ramachandran, Brian Williams, and Robert Benander of Ultramet for Marshall Space Flight Center. For more information, contact Sammy Nabors, MSFC Commercialization Assistance Lead, at sammy.a.nabors@nasa.gov. Refer to MFS-32736-1.*

## Process for Making a Noble Metal on Tin Oxide Catalyst

**This method produces an efficient, room-temperature catalyst for recombining carbon monoxide and oxygen products.**

*Langley Research Center, Hampton, Virginia*

To produce a noble metal-on-metal oxide catalyst on an inert, high-surface-area support material (that functions as a catalyst at approximately room temperature using chloride-free reagents), for use in a carbon dioxide laser, requires two steps: First, a commercially available, inert, high-surface-area support material (silica spheres) is coated with a thin layer of metal oxide, a monolayer equivalent. Very beneficial results have been obtained using nitric acid as an oxidizing agent because it leaves no residue. It is also helpful if the spheres are first de-aerated by boiling in water to allow the entire surface to be coated. A metal, such as tin, is then dissolved in the oxidizing agent/support material mixture to yield, in the case of tin, metastannic acid. Although tin has proven especially beneficial for use in a closed-cycle CO<sub>2</sub> laser, in general any metal with two valence states, such as most transition metals and antimony, may be used. The metastannic acid will be adsorbed onto the high-surface-area spheres, coating them. Any excess oxidizing agent is then evaporated, and the resulting metastan-

nic acid-coated spheres are dried and calcined, whereby the metastannic acid becomes tin(IV) oxide.

The second step is accomplished by preparing an aqueous mixture of the tin(IV) oxide-coated spheres, and a soluble, chloride-free salt of at least one catalyst metal. The catalyst metal may be selected from the group consisting of platinum, palladium, ruthenium, gold, and rhodium, or other platinum group metals. Extremely beneficial results have been obtained using chloride-free salts of platinum, palladium, or a combination thereof, such as tetraammineplatinum (II) hydroxide ([Pt(NH<sub>3</sub>)<sub>4</sub>](OH)<sub>2</sub>), or tetraamminepalladium nitrate ([Pd(NH<sub>3</sub>)<sub>4</sub>](NO<sub>3</sub>)<sub>2</sub>).

It is also beneficial if the coated spheres are first de-aerated by boiling. The platinum salt will be adsorbed onto the coated spheres. A chloride-free reducing agent is then added to the aqueous mixture whereby the catalyst metal is deposited on the tin(IV) oxide-coated spheres. Any reducing agent that decomposes to volatile products and water upon reaction or drying may be used.

Formic acid, hydroxylamine (NH<sub>2</sub>OH), hydrazine (N<sub>2</sub>H<sub>4</sub>), and ascorbic acid are particularly advantageous. After the metal has been deposited on the tin(IV) oxide-coated spheres, the solution is evaporated to dryness, whereby the desired noble metal-on-metal oxide catalyst is obtained.

This innovative process results in a more uniform application than other methods. Similarly, the method of forming and applying a precious metal to either tin oxide, or an inert substrate, is a one-step process and occurs at a lower temperature than that commonly used by other processes. This invention is inherently clean because excess reagents, such as nitric acid and formic acid, as well as unwanted products, such as nitrates and formates, all decompose and are removed from the system by simple evaporation without the necessity for separating them by filtration or washing.

*This work was done by Patricia Davis and Irvin Miller of Langley Research Center and Billy Upchurch of Science and Technology Corporation. Further information is contained in a TSP (see page 1). LAR-13741-1*



## Stacked Corrugated Horn Rings

NASA's Jet Propulsion Laboratory, Pasadena, California

This Brief describes a method of machining and assembly when the depth of corrugations far exceeds the width and conventional machining is not practical. The horn is divided into easily machined, individual rings with shoulders to control the depth. In this specific instance, each of the corrugations is identical in profile, and only differs in diameter and outer profile. The horn is segmented into rings

that are cut with an interference fit (zero clearance with all machining errors biased toward contact). The interference faces can be cut with a reverse taper to increase the holding strength of the joint. The taper is a compromise between the interference fit and the clearance of the two faces during assembly.

Each internal ring is dipped in liquid nitrogen, then nested in the previous,

larger ring. The ring is rotated in the nest until the temperature of the two parts equalizes and the pieces lock together. The resulting assembly is stable, strong, and has an internal finish that cannot be achieved through other methods.

*This work was done by John B. Sosnowski of Caltech for NASA's Jet Propulsion Laboratory. For more information, contact [iaoffice@jpl.nasa.gov](mailto:iaoffice@jpl.nasa.gov). NPO-47213*

## Refinements in an Mg/MgH<sub>2</sub>/H<sub>2</sub>O-Based Hydrogen Generator

Externally generated steam would be needed only briefly to start operation.

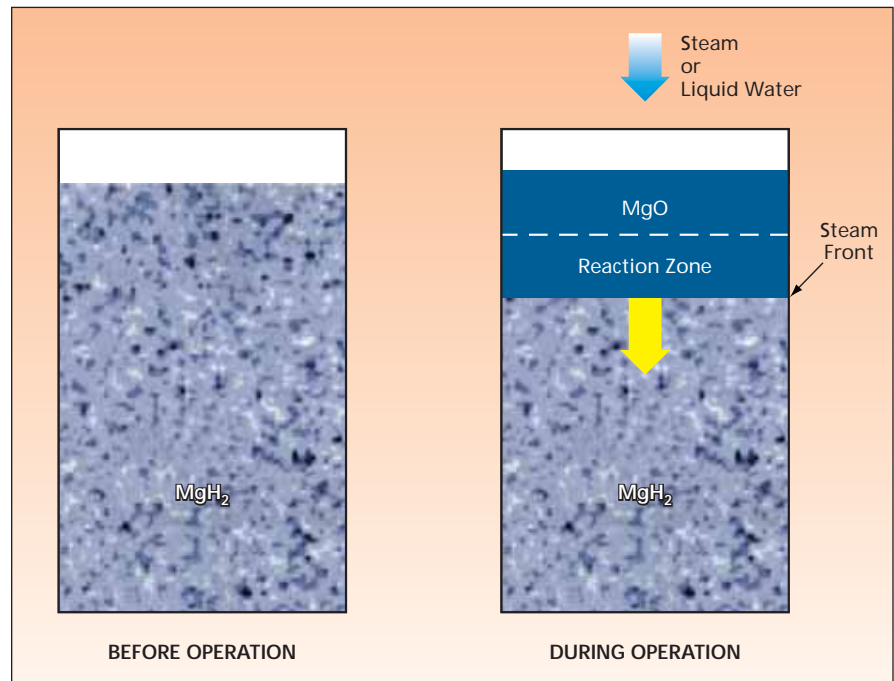
NASA's Jet Propulsion Laboratory, Pasadena, California

Some refinements have been conceived for a proposed apparatus that would generate hydrogen (for use in a fuel cell) by means of chemical reactions among magnesium, magnesium hydride, and steam. The refinements lie in tailoring spatial and temporal distributions of steam and liquid water so as to obtain greater overall energy-storage or energy-generation efficiency than would otherwise be possible.

A description of the prior art is prerequisite to a meaningful description of the present refinements. The hydrogen-generating apparatus in question is one of two versions of what was called the "advanced hydrogen generator" in "Fuel-Cell Power Systems Incorporating Mg-Based H<sub>2</sub> Generators" (NPO-43554), *NASA Tech Briefs*, Vol. 33, No. 1 (January 2009), page 52. To recapitulate: The apparatus would include a reactor vessel that would be initially charged with magnesium hydride. The apparatus would exploit two reactions:

- The endothermic decomposition reaction  $MgH_2 \rightarrow Mg + H_2$ , which occurs at a temperature  $\geq 300^\circ C$ , and
- The exothermic oxidation reaction  $MgH_2 + H_2O \rightarrow MgO + 2H_2$ , which occurs at a temperature  $\geq 330^\circ C$ .

Once the initial heating was complete and both reactions under way, the endothermic reaction would be sustained by the heat generated from the exothermic reaction. For every mole of MgH<sub>2</sub> oxidized, sufficient waste heat is



Water Would Be Injected at one end of a reactor bed containing MgH<sub>2</sub> particles. Initially, the water would be in the form of steam as needed to start the reactions. Thereafter, liquid water would be injected, and one of the reactions, which is exothermic, would supply the necessary heat.

generated to decompose an additional three moles of the hydride. As a consequence of these reaction ratios, the major reaction product is Mg, and the minor one MgO. Both have extremely low toxicity. MgH<sub>2</sub> is easily recycled to Mg. In theory, no energy is required because regeneration produces enough

heat to power the process. A practical system would not be 100-percent efficient so it would be expected that there would be a modest energy cost. The MgO can be safely and easily recycled in a magnesium-refining plant for less than the cost of smelting Mg because MgO is an intermediate product of that

process. This concludes the description of the prior art.

The present refinements reflect the following ideas: In principle, the design and operation of the reactor could be optimized in the sense that the rate of generation of heat in the exothermic reaction, the rate of consumption of heat in the endothermic reaction, and the flow of heat from the exothermic to the endothermic reaction could be tailored to minimize the input energy needed to produce a given amount of  $H_2$ . In turn, the reaction rates could be tailored by tailoring gradients of temperature and chemical composition, which, in turn, could be tailored through adjustments in rates of flow of steam and liquid water into the reactor, recognizing a need to adjust the rates because the gradients of

temperature and chemical composition evolve as  $MgH_2$  is consumed and  $MgO$  is generated.

For the purpose of illustrating the refinements, the figure schematically depicts a reactor that has a simple shape and inlets for steam and liquid water at one end only. One of the refinements would be to inject steam only at the beginning of operation, in no more than the quantity needed to initiate the exothermic reaction. The combination of heating and water vapor provided by steam would initiate both exothermic and endothermic reactions. With initiation of the exothermic reaction, sufficient heat is produced to allow the use of liquid water feed instead of steam. Some of the heat from the exothermic reaction would be consumed in heating

the liquid water to steam. As operation continued, the steam front and the hydrogen-generating region would move farther into the region initially containing  $MgH_2$ , leaving behind the  $MgO$  and  $Mg$  waste product. The rate of the exothermic reaction would be adjusted by adjusting the rate of injection of liquid water. If the reactor were of a more-complex configuration featuring multiple injection points, then the rates of injection of water at those points could be adjusted individually to obtain a more nearly optimum spatial and temporal distribution of temperature throughout the reactor.

*This work was done by Andrew Kindler and Yuhong Huang of Caltech for NASA's Jet Propulsion Laboratory. For more information, contact [iaoffice@jpl.nasa.gov](mailto:iaoffice@jpl.nasa.gov). NPO-46064*

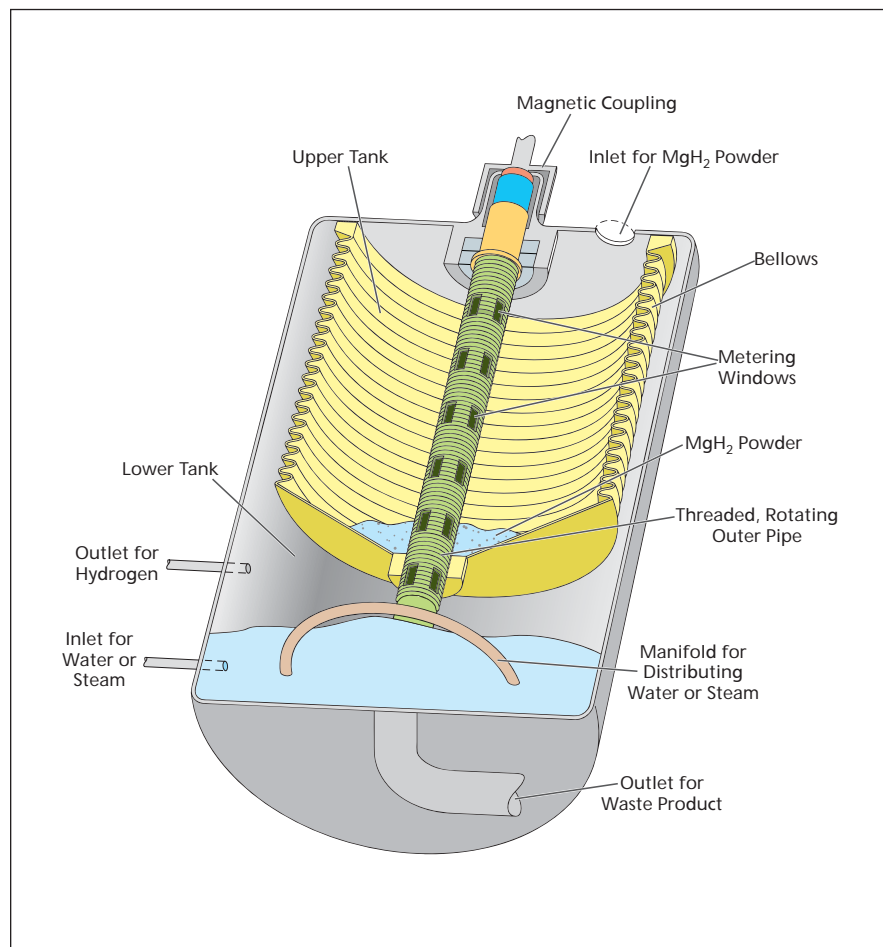
## ⚙️ Continuous/Batch $Mg/MgH_2/H_2O$ -Based Hydrogen Generator

Size and weight would be less than those of prior  $H_2$  generators.

*NASA's Jet Propulsion Laboratory, Pasadena, California*

A proposed apparatus for generating hydrogen by means of chemical reactions of magnesium and magnesium hydride with steam would exploit the same basic principles as those discussed in the immediately preceding article, but would be designed to implement a hybrid continuous/batch mode of operation. The design concept would simplify the problem of optimizing thermal management and would help to minimize the size and weight necessary for generating a given amount of hydrogen.

The apparatus would include a vessel, the interior volume of which would be divided into an upper and a lower tank (see figure). The upper tank would serve as a fuel-storage/feeder unit: It would include a bellows initially filled with  $MgH_2$  powder (the fuel), plus a mechanism that would include a rotating threaded outer pipe with metering windows and a non-rotating, non-threaded inner pipe with metering windows, for feeding the powder into the lower tank at a controlled rate. As the outer pipe was rotated, the windows in the pipes would alternately expose or occlude each other. The mechanism would be driven by an external motor via a magnetic coupling. The mechanism would also serve partly as a valve to prevent the undesired flow of steam from the reactor into the storage volume in



This Hydrogen Generator would function in a hybrid of batch and continuous modes.

that when powder was not being fed, the outer pipe would be rotated to a shaft angle at which the windows in the two pipes would occlude each other. The thread on the outer pipe would engage a threaded fitting on the bottom of the bellows, so that rotation of the outer pipe would compress the bellows as the powder was consumed.

The lower tank would serve as both a reactor and chamber for storing the solid waste end product (MgO) of the hydrogen-generating reactions. As the powder was fed from the upper tank to the lower tank and the bellows was compressed, the volume of the lower tank would grow, making room for the growing amount of waste material. Because fresh fuel would be dropped over the most recently reacted portion of the consumed fuel, it would always come in

contact with the hottest part. There would be ample time for the fuel to react as nearly completely as possible because once the fuel was in the reactor, it would stay there. A thermally insulating layer (not shown in the figure) on the bottom of the bellows would reduce the undesired flow of heat from the reactor to the storage volume, thereby helping to suppress undesired decomposition of the  $MgH_2$  in the storage volume.

As described thus far, the apparatus would operate in a batch mode. The upper tank could be refilled with  $MgH_2$  powder from the top, and the MgO solid waste could be removed from the bottom. However, it would be necessary to interrupt operation during such refilling and emptying and during concomitant reverse rotation of the

threaded outer pipe to reset the bellows to full storage volume. Thus, truly continuous operation would not be possible: The apparatus would operate in a quasi-batch, quasi-continuous mode.

*This work was done by Andrew Kindler and Yuhong Huang of Caltech for NASA's Jet Propulsion Laboratory.*

*In accordance with Public Law 96-517, the contractor has elected to retain title to this invention. Inquiries concerning rights for its commercial use should be addressed to:*

*Innovative Technology Assets Management  
JPL*

*Mail Stop 202-233*

*4800 Oak Grove Drive*

*Pasadena, CA 91109-8099*

*E-mail: iaoffice@jpl.nasa.gov*

*Refer to NPO-46058, volume and number of this NASA Tech Briefs issue, and the page number.*

---

## Strain System for the Motion Base Shuttle Mission Simulator

*Lyndon B. Johnson Space Center, Houston, Texas*

The Motion Base Shuttle Mission Simulator (MBSMS) Strain System is an innovative engineering tool used to monitor the stresses applied to the MBSMS motion platform tilt pivot frames during motion simulations in real time. The Strain System comprises hardware and software produced by several different companies. The system utilizes a series of strain gages, accelerometers, orientation sensor, rotational meter, scanners, computer, and software packages working in unison. By monitoring and recording the in-

puts applied to the simulator, data can be analyzed if weld cracks or other problems are found during routine simulator inspections. This will help engineers diagnose problems as well as aid in repair solutions for both current as well as potential problems.

The system is located with a line-of-sight to the Motion Base for real-time on-site monitoring. In addition to local monitoring, several off-site engineering computers are loaded with software allowing the user to remotely log onto the Strain System computer, monitor the sys-

tem, and adjust the software settings as required. Additional commercial software products have been programmed to automate the Strain System software. This removes the typical daily manual interaction required by the system to boot, record, stop, and save the resultant motion data for future analysis.

*This work was done by David C Huber, Karl G. Van Vossen, Glenn W. Kunkel, and Larry W. Wells of United Space Alliance for Johnson Space Center. Further information is contained in a TSP (see page 1). MSC 24386-1*

---

## Ko Displacement Theory for Structural Shape Predictions

**Prediction system enables real-time aero-elastic aircraft wing-shape control.**

*Dryden Flight Research Center, Edwards, California*

The development of the Ko displacement theory for predictions of structure deformed shapes was motivated in 2003 by the Helios flying wing, which had a 247-ft (75-m) wing span with wingtip deflections reaching 40 ft (12 m). The Helios flying wing failed in midair in June 2003, creating the need to develop new technology to predict in-flight deformed shapes of unmanned aircraft wings for visual display before the ground-based pilots.

Any types of strain sensors installed on a structure can only sense the surface

strains, but are incapable to sense the overall deformed shapes of structures. After the invention of the Ko displacement theory, predictions of structure deformed shapes could be achieved by feeding the measured surface strains into the Ko displacement transfer functions for the calculations of out-of-plane deflections and cross sectional rotations at multiple locations for mapping out overall deformed shapes of the structures. The new Ko displacement theory combined with a strain-sensing system

thus created a revolutionary new structure-shape-sensing technology.

The formulation of the Ko displacement theory stemmed from the integrations of the beam curvature equation (second order differential equation). The beamlike structure (wing) was first discretized into multiple small domains so that beam depth and surface strain distributions could be represented with piecewise linear functions. This discretization approach enabled piecewise integrations of the

beam curvature equation in closed forms to yield slope and deflection equations for each domain in recursion formats. The final deflection equations in summation forms (called Ko displacement transfer functions), which contain no structural properties (such as bending stiffness), were then expressed in terms of domain length, beam depth factor, and surface bending strains at the domain junctures. In fact, the effect of the structural properties is absorbed by surface strains.

For flying wing structures, the two-line strain-sensing system is a powerful method for simultaneously monitoring the bending and cross sectional rotations. The two-line strain-sensing system eliminates the need for installing the shear strain sensors to measure the surface distortions through which the wing structure cross sectional rotations could be determined.

The Ko displacement theory combined with onboard fiber-optic strain-sensing system forms a powerful tool

for in-flight deformed shape monitoring of flexible wings and tails, such as those often employed on unmanned flight vehicles by the ground-based pilot for maintaining safe flights. In addition, the real-time wing shape monitored could then be input to the aircraft control system for aero-elastic wing-shape control.

*This work was done by William L. Ko of Dryden Flight Research Center. Further information is contained in a TSP (see page 1). DRC-006-024*

---

## Pyrotechnic Actuator for Retracting Tubes Between MSL Subsystems

*NASA's Jet Propulsion Laboratory, Pasadena, California*

An apparatus, denoted the “retractuator” (a contraction of “retracting actuator”), was designed to help ensure clean separation between the cruise stage and the entry-vehicle subsystem of the Mars Science Laboratory (MSL) mission. The retractuator or an equivalent mechanism is needed because of tubes that (1) transport a heat-transfer fluid between the stages during flight and (2) are cut immediately prior to separation of the stages retractuator. The role of the retractuator is to retract the tubes, after

they are cut and before separation of the subsystem, so that cut ends of the tubes do not damage thermal-protection coats on the entry vehicle and do not contribute to uncertainty of drag and consequent uncertainty in separation velocity.

The retractuator was conceived as a less massive, less bulky, and more powerful alternative to a traditional spring-actuated retractor. The retractuator is a modified version of a prior pyrotechnically actuated cutter. The modifications include alterations of the geometries of

pyrotechnic charges, piston, and cylinder; replacing the cutter blade with a push rod; and other changes to reduce weight, arrest the piston at the end of its stroke, and facilitate installation.

*This work was done by John C. Gallon, Richard G. Webster, Keith D. Patterson, and Matthew A. Orzewalla of Caltech, Eric T. Roberts of Raytheon Co., and Andrew J. Tuszynski of Columbus Technologies and Services, Inc. for NASA's Jet Propulsion Laboratory. For more information, contact iaoffice@jpl.nasa.gov. NPO-45680*



## Surface-Enhanced X-Ray Fluorescence

**XRF spectra can be enhanced by large factors.**

*NASA's Jet Propulsion Laboratory, Pasadena, California*

Surface-enhanced x-ray fluorescence (SEn-XRF) spectroscopy is a form of surface-enhanced spectroscopy that was conceived as a means of obtaining greater sensitivity in x-ray fluorescence (XRF) spectroscopy. As such, SEn-XRF spectroscopy joins the ranks of such other, longer-wavelength surface-enhanced spectroscopies as those based on surface-enhanced Raman scattering (SERS), surface-enhanced resonance Raman scattering (SERRS), and surface-enhanced infrared Raman absorption (SEIRA), which have been described in previous *NASA Tech Briefs* articles.

XRF spectroscopy has been used in analytical chemistry for determining the elemental compositions of small samples. XRF spectroscopy is rapid and quantitative and has been applied to a variety of metal and mineralogical samples. The main drawback of XRF spectroscopy as practiced heretofore is that sensitivity has not been as high as required for some applications.

In SEn-XRF as in the other surface-enhanced spectroscopies, one exploits several interacting near-field phenomena, occurring on nanotextured surfaces, that give rise to local concentrations of incident far-field illumination. In this case, the far-field illumination comes from an x-ray source. Depending on the chemical composition and the geometry of a given nanotextured surface, these phenomena could include the lightning-rod effect (concentration of electric fields at the sharpest points on needlelike surface features), surface plasmon resonances, and grazing incidence geometric effects. In the far field, the observable effect of these phenomena is an increase in the intensity of the spectrum of interest — in this case, the x-ray fluorescence spectrum of chemical elements of interest that may be present within a surface layer at distances no more than a few nanometers from the surface.

In experiments, SEn-XRF was demonstrated on aluminum substrates, the surfaces of some of which had been randomly nanotextured (see Figure 1) by briefly etching them in hydrochloric

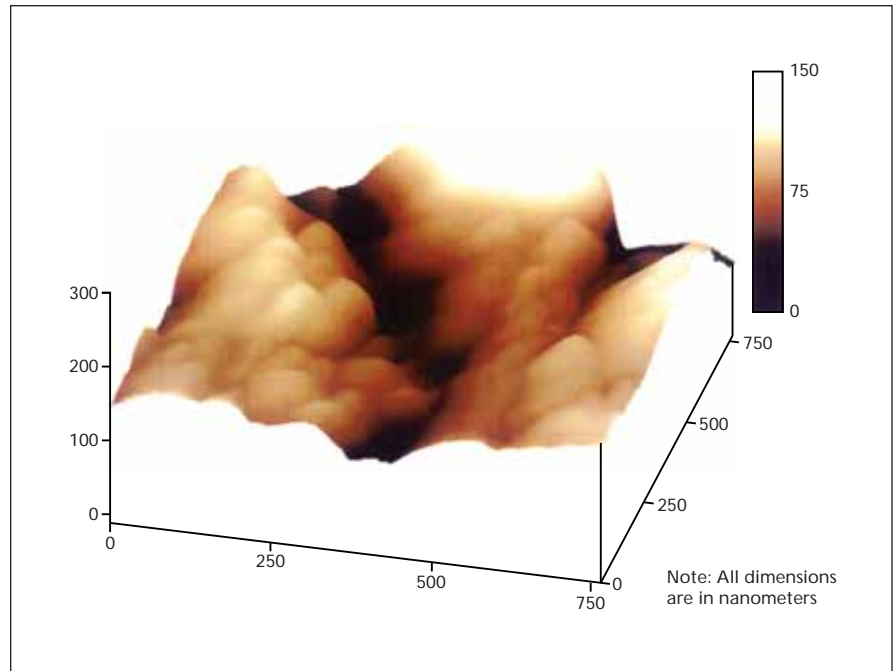


Figure 1. This Atomic-Force-Microscope Image shows a portion of the surface of an aluminum substrate that was roughened by a 1-minute etch in concentrated hydrochloric acid.

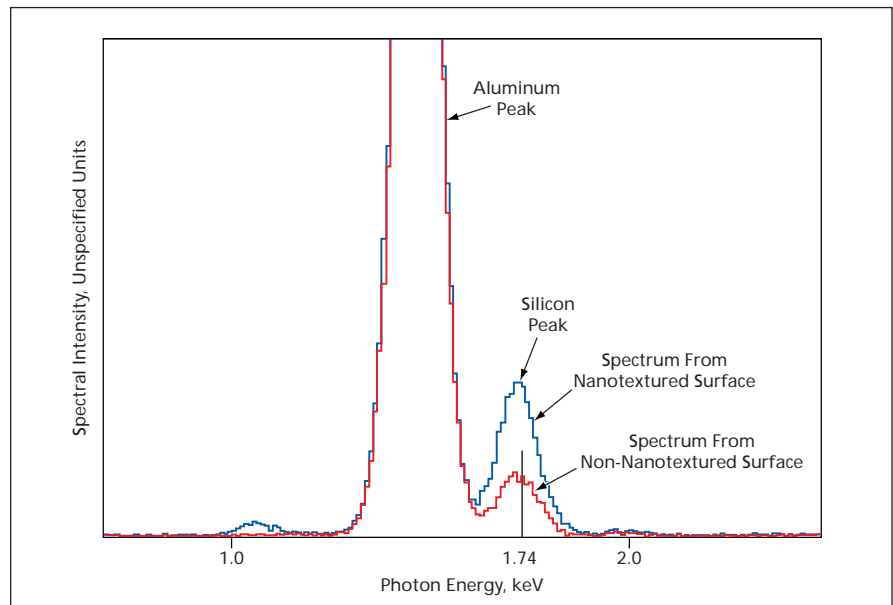


Figure 2. Silicon X-Ray Fluorescence Peaks at 1.74 keV were measured on aluminum surfaces coated with 340-nm-thick layers of silicone oil. The peak from the nanotextured surface was about 2.5 times as high as that from the nanotextured surface. Taking account of calculations showing that the enhancement occurs only within the 5-nm-thick sublayer closest to the surface, it was estimated that if the surfaces were coated to only 5-nm thickness, the factor of enhancement would be at least 170.

acid. Thin layers containing elements of interest (Si, I, K, Hg, and Pb) were deposited on the substrate, variously, from dilute salt solutions (in the case of K, Hg, and Pb), by vapor sublimation (in the case of I), or in a thin film of silicone oil (in the case of Si). XRF spectra of the thus-coated substrate surfaces were obtained by use of a commercial XRF microprobe instrument. In some cases, the XRF spectra of elements of interest on the nanotextured substrates were found

to be enhanced significantly over the spectra from the corresponding substrates that had not been nanotextured (for example, see Figure 2).

*This work was done by Mark Anderson of Caltech for NASA's Jet Propulsion Laboratory. Further information is contained in a TSP (see page 1).*

*In accordance with Public Law 96-517, the contractor has elected to retain title to this invention. Inquiries concerning rights for its commercial use should be addressed to:*

*Innovative Technology Assets Management  
JPL*

*Mail Stop 202-233  
4800 Oak Grove Drive  
Pasadena, CA 91109-8099  
(818) 354-2240*

*E-mail: iaoffice@jpl.nasa.gov*

*Refer to NPO-44351, volume and number of this NASA Tech Briefs issue, and the page number.*

---

## Infrared Sensor on Unmanned Aircraft Transmits Time-Critical Wildfire Data

**The sensor detects light at visible, infrared, and thermal wavelengths.**

*Dryden Flight Research Center, Edwards, California*

Since 2006, NASA's Dryden Flight Research Center (DFRC) and Ames Research Center have been perfecting and demonstrating a new capability for geolocation of wildfires and the real-time delivery of data to firefighters. Managed for the Western States Fire Mission, the Ames-developed Autonomous Modular Scanner (AMS), mounted beneath a wing of DFRC's MQ-9 Ikhana remotely piloted aircraft, contains an infrared sensor capable of discriminating temperatures within 0.5 °F ( $\approx 0.3$  °C), up to 1,000 °F ( $\approx 540$  °C).

The AMS operates like a digital camera with specialized filters to detect light energy at visible, infrared, and thermal wavelengths. By placing the AMS aboard unmanned aircraft, one can gather in-

formation and imaging for thousands of square miles, and provide critical information about the location, size, and terrain around fires to commanders in the field. In the hands of operational agencies, the benefits of this NASA research and development effort can support nationwide wildfire fighting efforts. The sensor also provides data for post-burn and vegetation regrowth analyses.

The MQ-9 Unmanned Aircraft System (UAS), a version of the Predator-B, can operate over long distances, staying aloft for over 24 hours, and controlled via a satellite-linked command and control system. This same link is used to deliver the fire location data directly to fire incident commanders, in less than 10 minutes from the time of overflight. In the

current method, similarly equipped short-duration manned aircraft, with limited endurance and range, must land, hand-carry, and process data, and then deliver information to the firefighters, sometimes taking several hours in the process. Meanwhile, many fires would have moved over great distances and changed direction. Speed is critical. The fire incident commanders must assess a very dynamic situation, and task resources such as people, ground equipment, and retardant-dropping aircraft, often in mountainous terrain obscured by dense smoke.

*This work was done by Mark Pestana of Dryden Flight Research Center. Further information is contained in a TSP (see page 1).  
DRC-010-020*

---

## Slopes To Prevent Trapping of Bubbles in Microfluidic Channels

**This idea helps to ensure functionality of micro-capillary electrophoresis devices.**

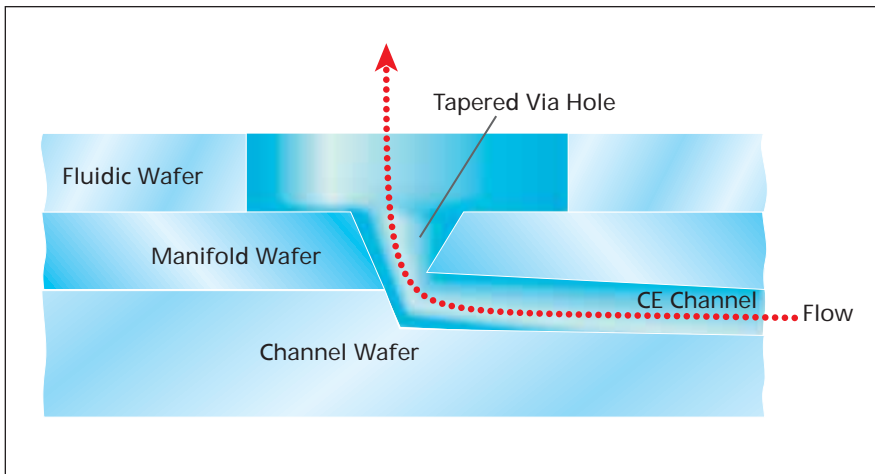
*NASA's Jet Propulsion Laboratory, Pasadena, California*

The idea of designing a microfluidic channel to slope upward along the direction of flow of the liquid in the channel has been conceived to help prevent trapping of gas bubbles in the channel. In the original application that gave rise to this idea, the microfluidic channels are parts of micro-capillary electrophoresis (microCE) devices undergoing development for use on Mars in detecting compounds indicative of life. It is necessary to prevent trapping of gas bubbles in these devices because unin-

terrupted liquid pathways are essential for sustaining the electrical conduction and flows that are essential for CE. The idea is also applicable to microfluidic devices that may be developed for similar terrestrial microCE biotechnological applications or other terrestrial applications in which trapping of bubbles in microfluidic channels cannot be tolerated.

A typical microCE device in the original application includes, among other things, multiple layers of borosilicate float glass wafers. Microfluidic channels

are formed in the wafers, typically by use of wet chemical etching. The figure presents a simplified cross section of part of such a device in which the CE channel is formed in the lowermost wafer (denoted the channel wafer) and, according to the present innovation, slopes upward into a via hole in another wafer (denoted the manifold wafer) lying immediately above the channel wafer. Another feature of the present innovation is that the via hole in the manifold wafer is made to taper to a wider



The slope of the CE Channel and the taper of the via hole in the manifold wafer help to prevent trapping of bubbles.

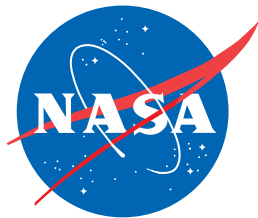
opening at the top to further reduce the tendency to trap bubbles.

At the time of reporting the information for this article, an effort to identify an optimum technique for forming the slope and the taper was in progress. Of the techniques considered thus far, the one considered to be most promising is precision milling by use of femtosecond laser pulses. Other similar techniques that may work equally well are precision milling using a focused ion beam, or a small diamond-tipped drill bit.

*This work was done by Harold F. Greer, Michael C. Lee, J. Anthony Smith, and Peter A. Willis of Caltech for NASA's Jet Propulsion Laboratory. For more information, contact [iaoffice@jpl.nasa.gov](mailto:iaoffice@jpl.nasa.gov). NPO-45934*







National Aeronautics and  
Space Administration